

Detachment of nanoparticles in granular media filtration

Ijung Kim¹, Tongren Zhu², Chan-Hoo Jeon³ and Desmond F. Lawler^{*4}

¹School of Urban and Civil Engineering, Hongik University, 94 Wausan-ro, Mapo-gu, Seoul, Republic of Korea

²Arcadis-US, Inc., 1717 West 6th Street, Ste. 210, Austin, TX 78703, USA

³Division of Marine Science, University of Southern Mississippi, Stennis Space Center, MS 39529, USA

⁴Department of Civil, Architectural and Environmental Engineering, The University of Texas at Austin, 1 University Station C1786, Austin, TX 78712, USA

(Received July 23, 2019, Revised November 14, 2019, Accepted November 18, 2019)

Abstract. An understanding of particle-particle interactions in filtration requires studying the detachment as well as the attachment of nanoparticles. Nanoparticles captured in a granular media filter can be released by changing the physicochemical factors. In this study, the detachment of captured silver nanoparticles (AgNPs) in granular media filtration was examined under different ionic strengths, ion type, and the presence or absence of natural organic matter (NOM). Filtration velocity and ionic strength were chosen as the physical and chemical factors to cause the detachment. Increasing filtration velocity caused a negligible amount of AgNP detachment. On the other hand, lowering ionic strength showed different release amounts depending on the background ions, implying a population of loosely captured particles inside the filter bed. Overall detachment was affected by ionic strength and ion type, and to a lesser degree by NOM coating which resulted in slightly more detachment (in otherwise identical conditions) than in the absence of that coating, possibly by steric effects. The secondary energy minimum with Na ions was deeper and wider than with Ca ions, probably due to the lack of complexation with citrate and charge neutralization that would be caused by Ca ions. This result implies that the change in chemical force by reducing ionic strength of Na ions could significantly enhance the detachment compared to that caused by a change in physical force, due to a weak electrostatic deposition between nanoparticles and filter media. A modification of the 1-D filtration model to incorporate a detachment term showed good agreement with experimental data; estimating the detachment coefficients for that model suggested that the detachment rate could be similar regardless of the amount of previously captured AgNPs.

Keywords: detachment; nanoparticles; secondary energy minimum; granular media filtration model

1. Introduction

The use of nanoparticles has increased in various areas such as medical (Farokhzad and Langer 2009, Bobo *et al.* 2016, Ramos *et al.* 2017, Kwon *et al.* 2018), material (Zhu *et al.* 2004, Berglund and Burgert 2018), cosmetics (Mu and Sprando 2010, Katz *et al.* 2015, Santos *et al.* 2019), and energy applications (Serrano *et al.* 2009, Lee *et al.* 2015, Zhe and Yuxiu 2018, Jun *et al.* 2019) and is expected to grow further in the near future (Zingg and Fischer 2019). Consequently, the release of nanoparticles to the environment from industrial sources or households can be anticipated (Nowack and Bucheli 2007, Benn *et al.* 2010, Nowack *et al.* 2016, Giese *et al.* 2018, Williams *et al.* 2019). Concerns about the potential harm from nanoparticles to humans and the environment are growing as the likelihood of exposure to nanoparticles becomes evident.

So far, the industrial sectors have focused on the beneficial uses of nanoparticles, which has contributed to the growth of nanotechnology, though the public perception on nanotechnology has more likely been negative as the demand for the regulation has grown (Larsson *et al.* 2019).

However, it should be noted that knowledge about nanoparticles can be selectively utilized by the people's viewpoint (Currall 2009). This lack of consensus on nanoparticles has made risk assessment and decision-making difficult. Therefore, a balanced evaluation of nanoparticles is still required.

Predicting human and environmental exposure to nanoparticles requires research on the transport of nanoparticles. A considerable amount of research has been conducted on the transport of nanoparticles in granular media filtration (Petosa *et al.* 2010, Molnar *et al.* 2015, Molnar *et al.* 2019). Since granular media filtration can mimic the soil or groundwater environment, it has been used to understand the migration of nanoparticles in such environments. Less attention has been given to the study of nanoparticle removal in granular media filtration at conditions reflecting drinking water and wastewater treatment.

Nanoparticle-filter media interaction can be divided into two sections; attachment and detachment. Most previous studies have focused on attachment. The effects of various particle characteristics (Lecoanet *et al.* 2004, Wang *et al.* 2012, Fan *et al.* 2015, Taghavy and Abriola 2018, Xia *et al.* 2019), solution chemistries (Solovitch *et al.* 2010, Xia *et al.* 2017, Kamrani *et al.* 2018, Xu *et al.* 2018), and operational conditions (Lecoanet and Wiesner 2004, Kim *et al.* 2017, Adrian *et al.* 2018) on attachment have been investigated.

*Corresponding author, Professor
E-mail: dlawler@mail.utexas.edu

Despite their tiny size, nanoparticles can be captured in granular media filter by controlling environmental conditions. However, the release of captured nanoparticles was reported when operational conditions changed chemically (e.g., ionic strength reduction (Franchi and O'Melia 2003, Tian *et al.* 2010, Dong *et al.* 2016, Wang *et al.* 2017, He *et al.* 2019, Liang *et al.* 2019), pH rise (Ryan and Elimelech 1996, Godinez and Darnault 2011), and cation exchange (Shen *et al.* 2012, Torkzaban *et al.* 2013, Zhang *et al.* 2018)). For particles larger than 2 μm , detachment also occurred by an increase in filtration velocity (Bergendahl and Grasso 2000, Torkzaban *et al.* 2015).

Generally, attachment and detachment are highly affected by electrostatic forces produced by the surface charges of particles. Based on DLVO theory (Derjaguin and Landau 1941, Verwey and Overbeek 1948), the interaction energy between a spherical particle and a planar surface can be expressed as the combination of electrostatic repulsion and van der Waals attraction. Such a net energy moves deeply downward (toward attraction) as the separation distance decreased to quite small values. This region is the primary energy minimum where the attachment becomes irreversible. As the separation distance increases, the net energy passes the peak repulsive energy point called the energy barrier in the case of unfavorable conditions, then further dips slightly into an attractive region. This second attractive region is known as the secondary energy minimum, where reversible attachment can occur. Detachment was believed to occur when attractive forces are weak in terms of electrostatic interaction, that is, when particles stay in the secondary energy minimum (Hahn and O'Melia 2004). However, this belief was challenged by Shen *et al.* (2012) who suggested a possible detachment from the primary energy minimum. All things considered, the exact mechanism is still unclear as to how nanoparticles are captured reversibly in granular media filters. Since detachment of nanoparticles in granular media filtration has not received much attention, detachment of nanoparticles under varying environmental conditions needs to be investigated.

This study selected silver nanoparticles (AgNPs) as the target material because they are the most widely used nanoparticles in consumer products. The objective of this study was to investigate the effect of physical and chemical forces on the detachment of AgNPs in granular media filtration. A series of laboratory scale granular media filtration tests was conducted under varying filtration velocities, ionic strengths, ion types, and the presence or absence of NOM to quantify the amounts of AgNPs captured and subsequently released when a physical or chemical condition was changed. Further, by assuming a homogeneous particle size and a spherical shape for the nanoparticles, the 1-D filtration model was explored to elucidate the detachment of AgNPs under various experimental conditions.

2. Theoretical calculations

Energy of interaction. The sum of the repulsive energy (V_R), attractive energy (V_A) and Born repulsion (V_B) was used to calculate the energy of interaction (Eqs. (1)-(3))

(Elimelech *et al.* 1995).

$$V_R = \pi \epsilon_0 \epsilon_r a_p \left(2\psi_{d_j} \psi_{d_p} \ln \left[\frac{1 + \exp(-\kappa s)}{1 - \exp(-\kappa s)} \right] + (\psi_{d_j}^2 + \psi_{d_p}^2) \ln [1 - \exp(-2\kappa s)] \right) \quad (1)$$

$$V_A = \frac{Aa_p}{6s} \left(1 + \frac{14s}{\lambda} \right)^{-1} \quad (2)$$

$$V_B = \frac{A\sigma_c^6}{7560} \left(\frac{8a_p + s}{(2a_p + s)^7} + \frac{6a_p - s}{s^7} \right) \quad (3)$$

Filtration model. Filtration models typically start from a one dimensional advection-diffusion equation, as described in Eq. (4), by assuming first order attachment kinetics (Li *et al.* 2008).

$$\frac{\partial N}{\partial t} = D \frac{\partial^2 N}{\partial x^2} - v_0 \frac{\partial N}{\partial x} - k_{att} N \quad (4)$$

N is the effluent number concentration at steady-state condition ($\#/L^3$), t is the time period after filtration starts (T), x is the distance from the surface of filter bed parallel to flow (L), D is the diffusion (plus dispersion) coefficient (L^2/T), and v_0 is the filtration velocity (L/T). The attachment coefficient (k_{att}) is calculated by Eq. (5) (Wang *et al.* 2008a):

$$k_{att} = \frac{v_0}{L} \ln \left(\frac{N_0}{N} \right) \quad (5)$$

L is filter depth (L), and N_0 is the initial AgNP number concentration ($\#/L^3$). To describe the detachment profile, the model was modified as shown in Eq. (6) by adding a term to include detachment from the solid-phase, dependent on the amount captured on the filter media (Wang *et al.* 2008b).

$$\frac{\partial N}{\partial t} = D \frac{\partial^2 N}{\partial x^2} - v_0 \frac{\partial N}{\partial x} - k_{att} N + k_{det} \frac{\rho_b}{\epsilon} S \quad (6)$$

k_{det} is the detachment coefficient (1/T), S is the specific deposit attached to the filter media ($\#/M$), ρ_b is the bulk density of the filter media (M/L^3), and ϵ is the volumetric water content, i.e., the porosity (-). S can be expressed in a whole filter as shown in Eq. (7):

$$S(x) = \frac{t_0 \epsilon k_{att} N_0}{\rho_b} \exp \left(-\frac{k_{att}}{v_0} x \right) \quad (7)$$

where t_0 is the AgNP injection period.

To solve Eq. (6), a numerical scheme that employs a finite difference method in space and the Crank-Nicolson method in time was used. In this study, the boundary and initial conditions were set as follows:

$$N(x=0, t < 30 \text{ min}) = N_0$$

$$N(x = 0, t \geq 30 \text{ min}) = 0$$

$$N(x, t = 0) = 0$$

Using the first order finite difference scheme of backward facing steps, this equation can be solved numerically using MATLAB (The MathWorks, Natick, MA).

3. Materials and methods

Citrate-capped AgNPs were purchased from Nanocomposix (San Diego, CA). Citrate was chosen because it is one of most commonly used capping agents in AgNP synthesis (Tolaymat *et al.* 2010). The laboratory analysis confirmed the spherical shape and the monodispersed size distribution of approximately 50 nm of AgNPs. To prevent any changes in AgNPs characteristics, the solution was kept at 4°C and away from light.

Spherical glass beads purchased from MO-SCI (St. Louis, MO) were used for filter media. The glass beads were mainly composed of SiO₂ and were sieved to a narrow size range between 300~350 μm. To remove impurities from the surface before use, the glass beads were subjected to an intensive washing procedure (Tobiason 1987).

Filtration experiments were conducted in a laboratory-scale acrylic cylindrical column. The inner diameter of the column was 3.81 cm and the depth of the filter bed was 10 cm. The porosity of the packed bed was determined gravimetrically to be 0.42. The two influent streams, AgNP suspension and background water, were separately prepared and pumped via a gear pump (Micropump, Cole Parmer) and a peristaltic pump (Easy-load II, Masterflex), respectively, and mixed immediately before entering into the column. The flow ratio of AgNP suspension to the background water was kept at 1:20 to maintain constant influent AgNP concentration.

The ionic strength was controlled by NaNO₃ or Ca(NO₃)₂ added to the background water. Since a sufficient amount of attachment is needed to achieve detachment, ionic strength of 100 mM with NaNO₃ and 10 mM with Ca(NO₃)₂ were chosen. In the experiments with NOM, Suwannee River Fulvic Acid (International Humic Substances Society, MN) was used to have 3.5 mg TOC/L background water to coat AgNPs and filter media. pH was controlled with 0.025 mM bicarbonate buffer at pH 7 to prevent significant changes in surface charge by pH. The filtration velocity was controlled at 2 m/hr, which is in the range used in conventional drinking water treatment plants, but far faster than groundwater flow.

Six filtration tests were conducted with varying ion types, ionic strengths, and/or filtration velocities (Table 1). Prior to the filtration test, the filter bed was flushed for 30 pore volumes by the background water. Each test consisted of three steps: 1) 25 pore volumes of filtration with AgNPs, 2) 25 pore volumes of flow at the same velocity and the same chemical conditions without AgNPs, and 3) 25 pore volumes of flow with either near zero ionic strength (deionized water) or with increased velocity. To achieve

Table 1 Summary of the filtration tests

Experiment #*	NOM coating	Ionic strength	Detachment
I10-Ca-I	No	10 mM Ca(NO ₃) ₂	Decreasing ionic strength
I10-Ca-FA-I	Yes	10 mM Ca(NO ₃) ₂	Decreasing ionic strength
I100-Na-I	No	100 mM NaNO ₃	Decreasing ionic strength
I10-Ca-V	No	10 mM Ca(NO ₃) ₂	Increasing velocity
I10-Ca-FA-V	Yes	10 mM Ca(NO ₃) ₂	Increasing velocity
I100-Na-V	No	100 mM NaNO ₃	Increasing velocity

*The I value is the ionic strength (mM), the chemical name is the source of the ionic strength, FA refers to fulvic acid coating, I refers to ionic strength reduction, and V refers to filtration velocity increase.

detachment of the captured AgNPs after 50 pore volumes, ionic strength was reduced to close to 0.025 mM or the filtration velocity was doubled from 2 to 4 m/hr. Samples were collected every 1 or 2 minutes during both filtration period and the detachment periods. AgNP samples were immediately acidified with trace metal grade HNO₃ to dissolve AgNPs (sample pH < 0.5). The acidified samples were stored at 4°C overnight. The dissolved Ag concentration was analyzed using an inductively coupled plasma-optical emission spectroscopy (ICP-OES, Varian). The surface charge of AgNPs and filter media was measured by electrophoretic light scattering (ELS, Malvern Zetasizer). Direct observations of AgNPs and filter media were conducted by transmission electron microscopy (TEM, FEI Tencai) and scanning electron microscopy (SEM, Zeiss).

4. Results and discussion

The experimental breakthrough curves are presented in terms of the relative concentration by pore volume (Fig. 1). Relative concentration is the normalized effluent concentration, or the fraction of the influent concentration remaining in the effluent. The detachment was relatively insignificant in all but one of the filtration tests. The most significant detachment occurred when the ionic strength was reduced from 100 mM NaNO₃ to near zero.

When the filtration velocity was doubled to allow a greater hydrodynamic drag force on the AgNPs already captured in the filter, there was only a negligible amount of AgNP detachment regardless of ionic strength, ion type, or NOM presence. Note that the required velocity to detach nanoparticles is theoretically considered to be more than 100 m/hr (Zhang 2012) which is far greater than any of those used in this study. Even with a wide and deep secondary energy minimum at I=100 mM of NaNO₃, the deposition is expected to be strong enough to withstand the hydrodynamic force applied in this study (though there was a tiny amount of detached AgNPs by the velocity change). This result does not refute the fact that hydrodynamic shear

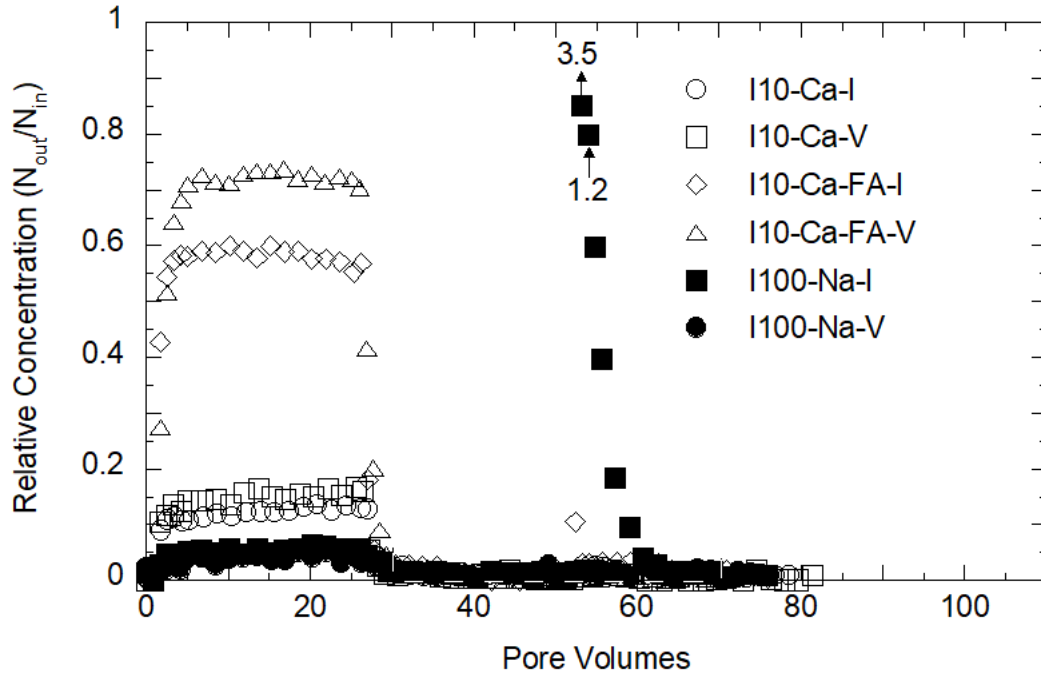


Fig. 1 Breakthrough curves of citrate AgNPs with detachment

Table 2 Percent of the originally attached AgNPs that became detached

Experiment #	I10-Ca-I	I10-Ca-V	I10-Ca-FA-I	I10-Ca-FA-V	I100-Na-I	I100-Na-V
Detached AgNPs/Attached AgNPs (%)	1.23	0.40	7.33	0.61	25.50	0.68

can affect the AgNPs deposited probably in the secondary energy minimum. However, it provides an insight that detachment can occur more easily with a chemical change rather than a physical one. In fact, more AgNPs can be attached at the leeward flow stagnation zone due to the local effect of hydrodynamic force (Chen *et al.* 2017). As long as the stagnation zone is available, the substantial AgNP detachment is unlikely to occur even at higher flow rates. The presence of such dead spaces indicates the spatial limitation of the hydrodynamic force in the AgNP release.

It should be noted that these filtration experiments were relatively short and designed primarily to test whether some of the capture of particles was in the range of the secondary minimum of the energy curve. The small amount of detachment with the velocity change in these experiments does not mean that detachment would not occur to a significant degree with the same velocity change after filtration of thousands of pore volumes (as occurs in water treatment practice). In that case, deposits might have significant thickness, and a change in the velocity could induce more detachment than seen in these experiments.

Even after the detachment period, AgNPs remained in the filter, yielding the amount of AgNPs that withstood the detachment condition. When the ionic strength was reduced, the remaining AgNPs in the filter were considered to be irreversibly attached in the primary energy minimum. In all

tests, the amount of AgNPs remaining in the filter (irreversibly attached) was quantified for the AgNP mass-balance. The ratio of the detached AgNPs to the originally attached AgNPs was calculated from the experimental data (and converted to a percent) and is shown in Table 2 for all of the experiments. The overall mass balance for each experiment is shown in Fig. 2.

In the case of the $I=100$ mM NaNO_3 test, the ratio of the detached to the originally attached AgNP mass was approximately 1:4. Assuming the detachment occurred for all particles attached in the secondary energy minimum, it suggests that one-fourth of AgNPs which could approach the primary energy minimum were stopped in the secondary energy minimum. Though the distance to the secondary energy minimum from the filter media surface was calculated to be only 4.19 nm (Table 3), the release of AgNPs seemed affected by the degree of the change from attraction to repulsion energy despite the small physical distance from the filter media. Also, since the influent AgNP concentration was in the low range (less than 100 $\mu\text{g/L}$), the number of the AgNPs injected to the filter was insufficient to fully cover every filter media surface. Therefore, multilayer AgNP deposition was unlikely to take place in this study. One might argue that $I=100$ mM of NaNO_3 could promote the aggregation of AgNPs in the suspension, leading to the deposition of AgNP aggregates on the filter media. However, the empty bed contact time was only approximately 1.18 min which is thought to be an insufficient time for AgNPs to be aggregated. Therefore, the significant amount of detachment is attributed to the detachment of the AgNPs that had been deposited in the secondary energy minimum.

With regard to the classical DLVO theory, the energy of the interaction between AgNPs and filter media was calculated (Fig. 3(a)). This calculation was conducted

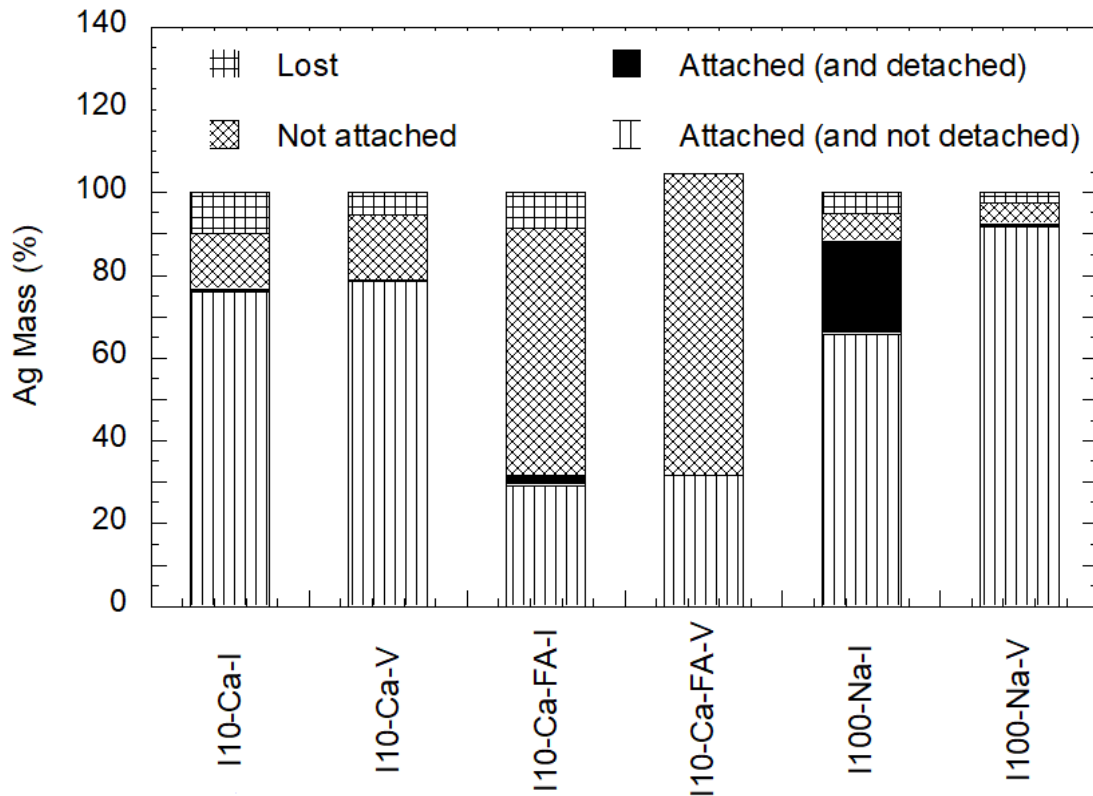


Fig. 2 Mass balance of Ag by mass in this study

Table 3 Results of the energy of interaction calculations

Experiment #	Surface potential at pH7 (mV)	Energy barrier height (J)	Energy barrier distance from surface (nm)	Secondary energy minimum depth (J)	Distance from the surface at the secondary energy minimum (nm)
I10-Ca-I	-20.26	1.08×10^{-20}	3.22	-1.62×10^{-21}	15.08
I10-Ca-FA-I	-16.20	7.01×10^{-21}	3.60	-1.70×10^{-21}	14.46
I100-Na-I	-50.75	2.81×10^{-20}	0.99	-1.18×10^{-20}	4.19

assuming a spherical particle and a flat plane since the size ratio of AgNP to filter media was close to 0.00015. A relatively deep and wide secondary energy minimum was calculated for the 100 mM NaNO_3 case while the other conditions showed no such significant secondary energy minimum. The surface potentials of AgNPs and glass beads were more negative at $I=100$ mM of NaNO_3 in comparison to the other two conditions, and that caused the greater repulsive energy reflected in the Fig. 3(a). The surface potentials for the three conditions were calculated from zeta-potential measurements and are shown in Table 3. It seems that the electric double layer suppression by the 100 mM ionic strength also led to the suppression of energy of interaction curves toward the filter media surface, resulting in a higher energy barrier and a deeper secondary energy minimum. Note that the secondary energy minimum disappeared when the ionic strength was greatly reduced, assuming the surface potentials of AgNPs and filter media were unaffected (Fig. 3(b)). Considering the experimental results for detachment in light of the energy interaction calculations, it is believed that the primary reason for AgNP detachment was their release from the secondary energy minimum.

A comparison of the detached AgNP amounts from I10-Ca-FA-I and I10-Ca-I (Fig. 2) shows that the NOM coating on the AgNP caused measurable detachment when the ionic strength was reduced. Since the location and the depth of the secondary energy minimum were almost identical regardless of NOM presence (Table 3), it is assumed that the steric effect rather than electrostatic effect by NOM coating might cause a weak AgNP deposition which is vulnerable to the ionic strength decrease. At $I=10$ mM of $\text{Ca}(\text{NO}_3)_2$, the steric effect by NOM coating appears to be the main factor because the surface charge becomes equalized regardless of the NOM coating due to Ca-citrate complexation, considering the higher affinity of citrate to Ca than Na (Walser 1961).

Nevertheless, the overall results highlighted that the change of ionic strength (which affects electrostatic repulsion) of Na ions had the most direct effect on the magnitude of detachment of AgNPs.

The filtration model derived from 1-D advection-diffusion equation was used as a tool to model the effluent profile of AgNPs, and all model outputs in this study were the concentrations at the outlet of the filter. This model was

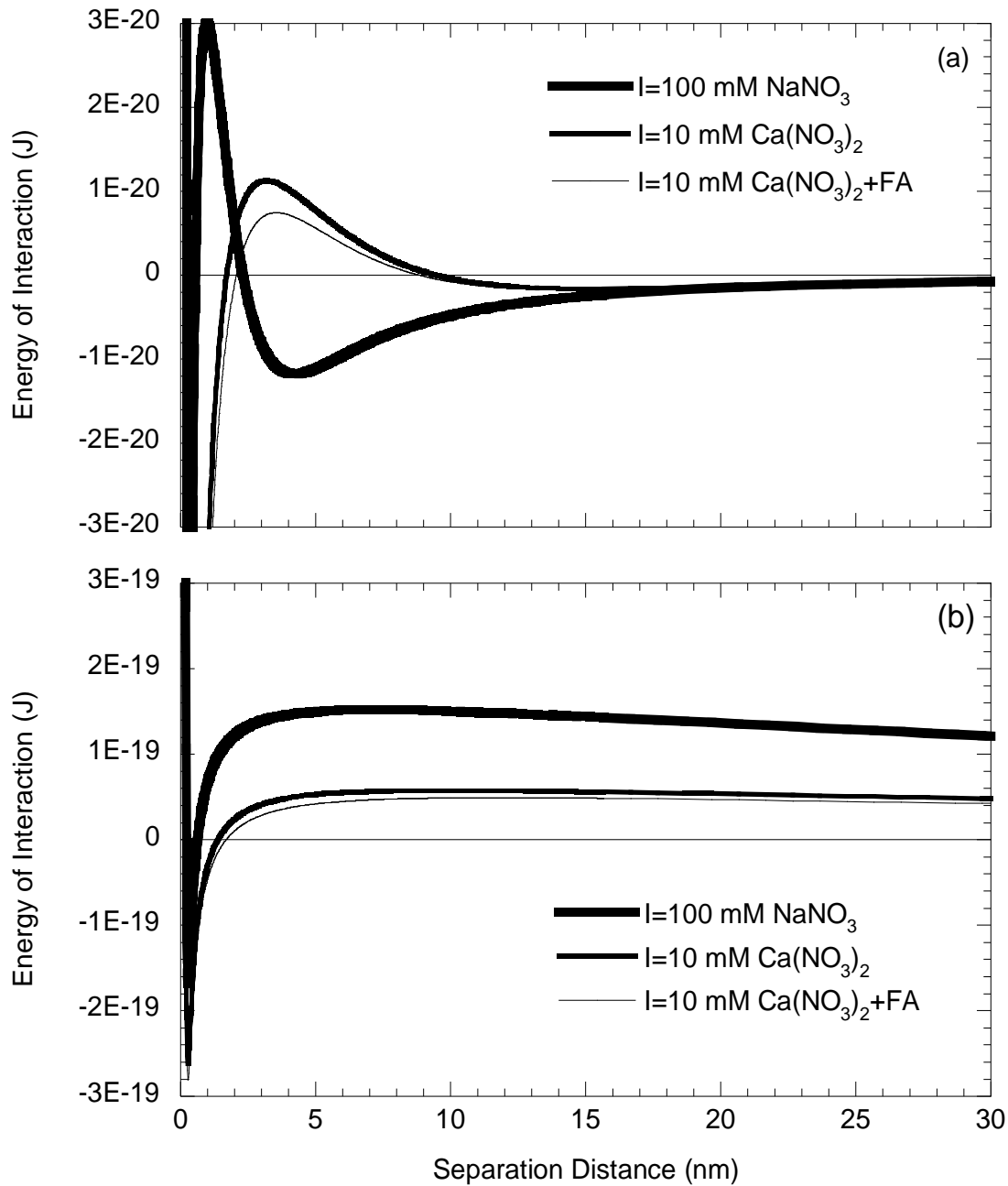


Fig. 3 Energy of interaction between citrate AgNPs and filter media (a) at the ionic strength during filtration and (b) at the low (near zero) ionic strength during the detachment phase of the experiments (at pH 7)

Table 4 Estimated detachment coefficients from six filtration tests

Experiment #	I10-Ca-I	I10-Ca-V	I10-Ca-FA-I	I10-Ca-FA-V	I100-Na-I	I100-Na-V
k_{det} (10^{-4} s^{-1})	0.018	0.69	0.82	0.016	0.17	0.0032

run by using the known value of v_0 and calculating k_{att} , and S directly from the experimental results from the attachment period. The diffusion plus dispersion coefficient was taken to be the particle diffusion coefficient, even though dispersion was probably greater than this value; the primary reason for using the model was to estimate the detachment coefficient, so this choice for the diffusion coefficient was

deemed unimportant. The remaining parameter, k_{det} was estimated to fit the model to the experimental result during the detachment period between 50 and 60 pore volumes. Overall, this model effectively simulated the sharp increase and decrease of citrate AgNPs in the experiments (Fig. 4). The assumption of first order attachment kinetics was reasonable because the surface area of filter media is substantially greater than the surface area of injected AgNPs. Also, the k_{det} derived in each test condition allowed good agreement with experimental results. This result demonstrates that the transport of 50 nm AgNPs in granular media filtration was primarily affected by diffusion and advection and that 1-D advection-diffusion equation was applicable to the conditions of the experiments.

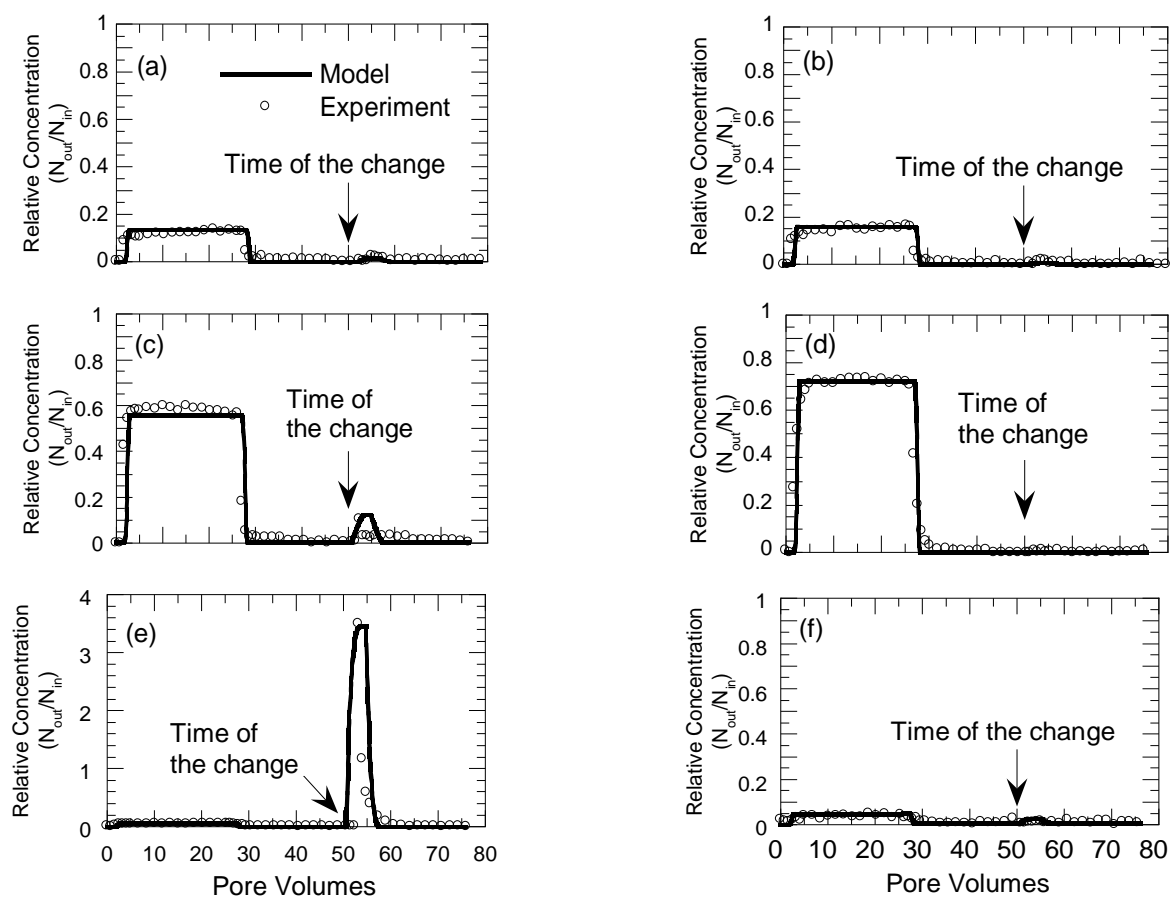


Fig. 4 Comparison of experimental results and model predictions for all filtration tests. Each column shows the cases of the detachment caused by ionic strength reduction (left) or by filtration velocity increase (right). Experimental condition varies from top to bottom (top: $I=10$ mM $\text{Ca}(\text{NO}_3)_2$, middle: $I=10$ mM $\text{Ca}(\text{NO}_3)_2$ with fulvic acid, bottom: $I=100$ mM NaNO_3)

This model was fitted to the detachment profile for each experimental condition. Values of k_{det} were estimated using the root-mean-square error in the short detachment period (50~60 pore volumes), and they are shown in Table 4.

At higher pore volume values, the detachment coefficient was estimated to be as low as 10^{-7} s^{-1} which indicates almost no detachment. The likelihood of further detachment after the first ten pore volumes of the detachment period was insubstantial because the detachment might be caused solely by eliminating the secondary energy minimum whose effect appeared immediately, just as turning off a switch.

Interestingly, the detachment coefficients from the two tests with the most detachment ($I=10$ mM of $\text{Ca}(\text{NO}_3)_2$ with fulvic acid and $I=100$ mM of NaNO_3 without NOM) were estimated to be similar, even though the amount of detached AgNPs was significantly different between those tests. The seemingly identical detachment coefficient with different amount of detachment was attributed to the different amounts of attachment. In other words, the detachment coefficient is the parameter which determines the detachment rate of a system independent of the amount of attachment. The similarity of results in these two experiments suggests that the steric effect by NOM coating causes as much detachment potential as the elimination of

secondary energy minimum. Thus, the detachment coefficient is a preferred parameter to interpret the detachment potential from different experimental conditions.

5. Conclusions

In this study, the detachment of AgNPs could be attributed mainly to the secondary energy minimum in terms of the amount of the detached AgNPs. The significant reduction in ionic strength resulted in effective detachment by eliminating the secondary energy minimum. Less detachment was observed with $I=10$ mM of $\text{Ca}(\text{NO}_3)_2$ than $I=100$ mM of NaNO_3 because Ca ions were able to effectively neutralize the surface charges, presumably by Ca-citrate complexation. The steric effect by NOM coating could lead to a weak AgNP deposition resulting in more detachment than in the absence of NOM. The velocity increase showed a negligible effect on the detachment because the velocity range applied here was much lower than the velocity level required to enable nanoparticle detachment. The remaining AgNPs after filtration and after a sudden decrease of the ionic strength was applied were considered to be irreversibly deposited in the primary energy minimum. The model derived from 1-D advection-

diffusion equation with attachment and detachment terms was successfully used to fit to the experimental results and estimate the detachment coefficients. The detachment occurred rapidly in a brief period immediately after the ionic strength decreased or filtration velocity increased, and the detachment coefficients were estimated using data from that period. The comparison of the detachment coefficients demonstrated the contribution of the steric effect to detachment.

References

- Adrian, Y.F., Schniedewind, U., Bradford, S.A., Simunek, J., Fernandez-Steeger, T.M. and Azzam, R. (2018), "Transport and retention of surfactant- and polymer-stabilized engineered silver nanoparticles in silicate-dominated aquifer material", *Environ. Pollut.*, **236**, 195-207. <https://doi.org/10.1016/j.envpol.2018.01.011>.
- Benn, T., Cavanagh, B., Hristovski, K., Posner, J.D. and Westerhoff, P. (2010), "The release of nanosilver from consumer products used in the home", *J. Environ. Quality*, **39**(6), 1875-1882. <https://doi.org/10.2134/jeq2009.0363>.
- Bergendahl, J. and Grasso, D. (2000), "Prediction of colloid detachment in a model porous media: hydrodynamics", *Chem. Eng. Sci.*, **55**(9), 1523-1532. [https://doi.org/10.1016/S0009-2509\(99\)00422-4](https://doi.org/10.1016/S0009-2509(99)00422-4).
- Berglund, L. A. and Burgert, I. (2018), "Bioinspired wood nanotechnology for functional materials", *Adv. Mater.*, **30**(19), 1704285. <https://doi.org/10.1002/adma.201704285>.
- Bobo, D., Robinson, K.J., Islam, J., Thurecht, K.J. and Corrie, S.R. (2016), "Nanoparticle-based medicines: A review of FDA-approved materials and clinical trials to date", *Pharmaceutical Res.*, **33**(10), 2373-2387. <https://doi.org/10.1007/s11095-016-1958-5>.
- Chen, C., Waller, T. and Walker, S.L. (2017), "Visualization of transport and fate of nano and micro-scale particles in porous media: modeling coupled effects of ionic strength and size", *Environ. Sci.: Nano*, **4**, 1025-1036. <https://doi.org/10.1039/C6EN00558F>.
- Currall, S.C. (2009), "Nanotechnology and society: New insights into public perceptions", *Nature Nanotechnology*, **4**, 79-80. <https://doi.org/10.1038/nnano.2008.423>.
- Derjaguin, B.V. and Landau, L. (1941), "The theory of stability of highly charged lyophobic sols and coalescence of highly charged particles in electrolyte solutions", *Acta Physicochim. URSS*, **14**, 633-652.
- Dong, S., Shi, X., Gao, B., Wu, J., Sun, Y., Guo, H., Xu, H. and Wu, J. (2016), "Retention and release of graphen oxide in structured heterogeneous porous media under saturated and unsaturated conditions", *Environ. Sci. Technol.*, **50**(19), 10397-10405. <https://doi.org/10.1021/acs.est.6b01948>.
- Elimelech, M., Jia, X., Gregory, J. and Williams, R. (1995), *Particle Deposition and Aggregation: Measurement, Modelling and Simulation*, (1st edition), Butterworth-Heinemann, Oxford, United Kingdom.
- Fan, W., Jiang, X.H., Yang, W., Geng, Z., Huo, M.X., Liu, Z.M. and Zhou, H. (2015), "Transport of graphen oxide in saturated porous media: Effect of cation composition in mixed Na-Ca electrolyte systems", *Sci. Total Environ.*, **511**, 509-515. <https://doi.org/10.1016/j.scitotenv.2014.12.099>.
- Farokhzad, O.C. and Langer, R. (2009), "Impact of nanotechnology on drug Delivery", *ACS Nano*, **3**(1), 16-20. <https://doi.org/10.1021/nn900002m>.
- Franchi, A. and O'Melia, C.R. (2003), "Effects of natural organic matter and solution chemistry on the deposition and reentrainment of colloids in porous media", *Environ. Sci. Technol.*, **37**(6), 1122-1129. <https://doi.org/10.1021/es015566h>.
- Giese, B., Klaessig, F., Park, B., Kaegi, R., Steinfeldt, M., Wigger, H., von Gleich, A. and Gottschalk, F. (2018), "Risks, release and concentrations of engineered nanomaterial in the environment", *Scientific Reports*, **8**, 1565. <https://doi.org/10.1038/s41598-018-19275-4>.
- Godinez, I.G. and Darnault, C.J.G. (2011), "Aggregation and transport of nano-TiO₂ in saturated porous media: Effects of pH, surfactants and flow velocity", *Water Res.*, **45**, 839-851. <https://doi.org/10.1016/j.watres.2010.09.013>.
- Hahn, M.W. and O'Melia, C.R. (2004), "Deposition and reentrainment of Brownian particles in porous media under unfavorable chemical conditions: Some concepts and applications", *Environ. Sci. Technol.*, **38**(1), 210-220. <https://doi.org/10.1021/es030416n>.
- He, J., Wang, D., Zhang, W. and Zhou, D. (2019), "Deposition and release of carboxylated graphene in saturated porous media: Effect of transient solution chemistry", *Chemosphere*, **235**, 643-650. <https://doi.org/10.1016/j.chemosphere.2019.06.187>.
- Jaisi, D.P., Saleh, N.B., Blake, R.E. and Elimelech, M. (2008), "Transport of single-walled carbon nanotubes in porous media: Filtration mechanisms and reversibility", *Environ. Sci. Technol.*, **42**(22), 8317-8323. <https://doi.org/10.1021/es801641v>.
- Jun, B.M., Kim, S., Heo, J., Park, C.M., Her, N., Jang, M., Huang, L., Han, J. and Yoon, Y. (2019), "Review of MXenes as new nanomaterials for energy storage/delivery and selected environmental applications", *Nano Res.*, **12**(3), 471-487. <https://doi.org/10.1007/s12274-018-2225-3>.
- Kamrani, S., Rezaei, M., Kord, M. and Baalousha, M. (2018), "Transport and retention of carbon dots (CDs) in saturated and unsaturated porous media: Role of ionic strength, pH, and collector grain size", *Water Res.*, **133**, 338-347. <https://doi.org/10.1016/j.watres.2017.08.045>.
- Katz, L.M., Dewan, K. and Bronaugh, R.L. (2015), "Nanotechnology in cosmetics", *Food Chem. Toxicology*, **85**, 127-137. <https://doi.org/10.1016/j.fct.2015.06.020>.
- Kim, I., Zhu, T., Youn, S. and Lawler, D.L. (2017), "Polymer-capped nanoparticle transport in granular media filtration: Deviation from the colloidal filtration model", *J. Environ. Eng.*, **143**(7), 03117003. [https://doi.org/10.1061/\(ASCE\)EE.1943-7870.0001228](https://doi.org/10.1061/(ASCE)EE.1943-7870.0001228).
- Kwon, H.J., Shin, K., Soh, M., Chang, H., Kim, J., Lee, J., Ko, G., Kim, B.H., Kim, D. and Hyeon, T. (2018), "Large-scale synthesis and medical applications of uniform-sized metal oxide nanoparticles", *Adv. Mater.*, **30**(42), 1704290. <https://doi.org/10.1002/adma.201704290>.
- Larsson, S., Jansson, M. and Boholm, A. (2019), "Expert stakeholders' perception of nanotechnology: risk, benefit, knowledge, and regulation", *J. Nanoparticle Res.*, **21**, 57. <https://doi.org/10.1007/s11051-019-4498-1>.
- Lecoanet, H.F., Bottero, J.Y. and Wiesner, M.R. (2004), "Laboratory assessment of the mobility of nanomaterials in porous media", *Environ. Sci. Technol.*, **38**(19), 5164-5169. <https://doi.org/10.1021/es0352303>.
- Lecoanet, H.F. and Wiesner, M.R. (2004), "Velocity effects on fullerene and oxide nanoparticle deposition in porous media", *Environ. Sci. Technol.*, **38**(16), 4377-4382. <https://doi.org/10.1021/es035354f>.
- Lee, Y.C., Lee, K. and Oh, Y.K. (2015), "Recent nanoparticle engineering advances in microalgal cultivation and harvesting processes of biodiesel production: A review", *Bioresource Technol.*, **184**, 63-72. <https://doi.org/10.1016/j.biortech.2014.10.145>.
- Li, Y.S., Wang, Y.G., Pennell, K.D. and Abriola, L.M. (2008), "Investigation of the transport and deposition of fullerene (C₆₀) nanoparticles in quartz sands under varying flow conditions", *Environ. Sci. Technol.*, **42**(19), 7174-7180. <https://doi.org/10.1021/es801305y>.

- Liang, Y., Bradford, S.A., Simunek, J. and Klumpp, E. (2019), "Mechanisms of graphene oxide aggregation, retention, and release in quartz sand", *Sci. Total Environ.*, **656**, 70-79. <https://doi.org/10.1016/j.scitotenv.2018.11.258>.
- Molnar, I.L., Johnson, W.P., Gerhard, J.I., Willson, C.S. and O'Carroll, D.M. (2015), "Predicting colloid transport through saturated porous media: A critical review", *Water Resources Res.*, **51**(9), 6804-6845. <https://doi.org/10.1002/2015WR017318>.
- Molnar, I.L., Pensini, E., Asad, M.A., Mitchell, C.A., Nitsche, L.C., Pyrak-Nolte, L.J., Mino, G.L. and Krol, M.M. (2019), "Colloid transport in porous media: A review of classical mechanisms and emerging topics", *Transport in Porous Media*, **130**(1), 129-156. <https://doi.org/10.1007/s11242-019-01270-6>.
- Mu, L. and Sprando, R.L. (2010), "Application of nanotechnology in cosmetics", *Pharmaceutical Res.*, **27**(8), 1746-1749. <https://doi.org/10.1007/s11095-010-0139-1>.
- Nowack, B. and Bucheli, T.D. (2007), "Occurrence, behavior and effects of nanoparticles in the environment", *Environ. Pollut.*, **150**(1), 5-22. <https://doi.org/10.1016/j.envpol.2007.06.006>.
- Nowack, B., Boldrin, A., Caballero, A., Hansen, S.F., Gottschalk, F., Heggelund, L., Hennig, M., Mackevica, A., Maes, H., Navratilova, J., Neubauer, N., Peters, R., Rose, J., Schaffer, A., Scifo, L., van Leeuwen, S., von der Kammer, F., Wohlleben, W., Wyrwoll, A. and Hristozov, D. (2016), "Meeting the needs for released nanomaterials required for further testing-The SUN Approach", *Environ. Sci. Technol.*, **50**(6), 2747-2753. <https://doi.org/10.1021/acs.est.5b04472>.
- Petosa, A.R., Jaisi, D.P., Quevedo, I.R., Elimelech, M. and Tufenkji, N. (2010), "Aggregation and deposition of engineered nanomaterials in aquatic environments: Role of physicochemical interactions", *Environ. Sci. Technol.*, **44**(17), 6532-6549. <https://doi.org/10.1021/es100598h>.
- Ramos, A. P., Crus, M. A. E., Tovani, C. B. and Ciancaglini, P. (2017), "Biomedical applications of nanotechnology", *Biophys. Rev.*, **9**(2), 79-89. <https://doi.org/10.1007/s12551-016-0246-2>.
- Ryan, J.N. and Elimelech, M. (1996), "Colloid mobilization and transport in groundwater", *Colloids Surfaces A Physicochem. Eng. Aspects*, **107**, 1-56. [https://doi.org/10.1016/0927-7757\(95\)03384-X](https://doi.org/10.1016/0927-7757(95)03384-X).
- Saleh, N., Kim, H.J., Phenrat, T., Matyjaszewski, K., Tilton, R.D. and Lowry, G.V. (2008), "Ionic strength and composition affect the mobility of surface-modified Fe-0 nanoparticles in water-saturated sand columns", *Environ. Sci. Technol.*, **42**(9), 3349-3355. <https://doi.org/10.1021/es071936b>.
- Santos, A.C., Morais, F., Simoes, A., Pereira, I., Sequeira, J.A.D. and Pereira-Silva, M. (2019), "Nanotechnology for the development of new cosmetic formulations", *Expert Opinion Drug Delivery*, **16**(4), 313-330. <https://doi.org/10.1080/17425247.2019.1585426>.
- Serrano, E., Rus, G. and Garcia-Martinez, J. (2009), "Nanotechnology for sustainable energy", *Renewable Sustainable Energy Rev.*, **13**(9), 2373-2384. <https://doi.org/10.1016/j.rser.2009.06.003>.
- Shen, C.Y., Lazouskaya, V., Jin, Y., Li, B.G., Ma, Z.Q., Zheng, W.J. and Huang, Y.F. (2012), "Coupled factors influencing detachment of nano- and micro-sized particles from primary minima", *J. Contaminant Hydrology*, **134**, 1-11. <https://doi.org/10.1016/j.jconhyd.2012.04.003>.
- Solovitch, N., Labille, J., Rose, J., Chaurand, P., Borschneck, D., Wiesner, M.R. and Bottero, J.Y. (2010), "Concurrent aggregation and deposition of TiO₂ nanoparticles in a sandy porous media", *Environ. Sci. Technol.*, **44**(13), 4897-4902. <https://doi.org/10.1021/es1000819>.
- Taghavy, A. and Abriola, L.M. (2018), "Modeling reactive transport of polydisperse nanoparticles: Assessment of the representative particle approach", *Environ. Sci.: Nano*, **5**, 2293-2303. <https://doi.org/10.1039/C8EN00666K>.
- Tian, Y., Gao, B., Silvera-Batista, C. and Ziegler, K.J. (2010), "Transport of engineered nanomaterials in saturated porous media", *J. Nanoparticle Res.*, **12**(7), 2371-2380. <https://doi.org/10.1007/s11051-010-9912-7>.
- Tobiason, J.E. (1987), "Physicochemical aspects of particle deposition in porous media", Ph.D. Dissertation; Johns Hopkins University, Baltimore, U.S.A.
- Tolaymat, T.M., El Badawy, A.M., Genaidy, A., Scheckel, K.G., Luxton, T.P. and Suidan, M. (2010), "An evidence-based environmental perspective of manufactured silver nanoparticle in syntheses and applications: A systematic review and critical appraisal of peer-reviewed scientific papers", *Sci. Total Environ.*, **408**(5), 999-1006. <https://doi.org/10.1016/j.scitotenv.2009.11.003>.
- Torkzaban, S., Bradford, S.A., Wan, J., Tokunaga, T. and Masoudih, A. (2013), "Release of quantum dot nanoparticles in porous media: Role of cation exchange and aging time", *Environ. Sci. Technol.*, **47**(20), 11528-11536. <https://doi.org/10.1021/es402075f>.
- Torkzaban, S., Bradford, S.A., Vanderzalm, J.L., Patterson, B.M., Harris, B. and Prommer, H. (2015), "Colloid release and clogging in porous media: Effects of solution ionic strength and flow velocity", *J. Contaminant Hydrology*, **181**, 161-171. <https://doi.org/10.1016/j.jconhyd.2015.06.005>.
- Verwey, E. and Overbeek, J.T.G. (1948), *Theory of The Stability of Lyophobic Colloids*, Elsevier, Amsterdam, The Netherlands.
- Walser, M. (1961), "Ion Association .5. Dissociation constants for complexes of citrate with sodium, potassium, calcium, and magnesium ions", *J. Physical Chem.*, **65**(1), 159-161. <https://doi.org/10.1021/j100819a045>.
- Wang, C., Bobba, A.D., Attinti, R., Shen, C., Lazouskaya, V., Wang, L.P. and Jin, Y. (2012), "Retention and transport of silica nanoparticles in saturated porous media: Effect of concentration and particle size", *Environ. Sci. Technol.*, **46**(13), 7151-7158. <https://doi.org/10.1021/es300314n>.
- Wang, D., Shen, C., Su, C., Chu, L. and Zhou, D. (2017), "Role of solution chemistry in the retention and release of graphene oxide nanomaterials in uncoated and iron oxide-coated sand", *Sci. Total Environ.*, **579**, 776-785. <https://doi.org/10.1016/j.scitotenv.2016.11.029>.
- Wang, P., Shi, Q.H., Liang, H.J., Steuerma, D.W., Stucky, G.D. and Keller, A.A. (2008a), "Enhanced environmental mobility of carbon nanotubes in the presence of humic acid and their removal from aqueous solution", *Small*, **4**(12), 2166-2170. <https://doi.org/10.1002/sml.200800753>.
- Wang, Y.G., Li, Y.S., Fortner, J.D., Hughes, J.B., Abriola, L.M. and Pennell, K.D. (2008b), "Transport and retention of nanoscale C₆₀ aggregates in water-saturated porous media", *Environ. Sci. Technol.*, **42**(10), 3588-3594. <https://doi.org/10.1021/es800128m>.
- Williams, R., Harrison, S., Keller, V., Kuenen, J., Lofts, S., Praetorius, A., Svendsen, C., Vermeulen, L.C. and van Wijnen, J. (2019), "Models for assessing engineered nanomaterial fate and behaviour in the aquatic environment", *Current Opinion in Environ. Sustainability*, **36**, 105-115. <https://doi.org/10.1016/j.cosust.2018.11.002>.
- Xia, T., Qu, Y., Liu, J., Qi, Z., Chen, W. and Wiesner, M.R. (2017), "Cation-inhibited transport of graphene oxide nanomaterials in saturated porous media: The Hofmeister effects", *Environ. Sci. Technol.*, **51**(2), 828-837. <https://doi.org/10.1021/acs.est.6b05007>.
- Xia, T., Ma, P., Qi, Y., Zhu, L., Qi, Z. and Chen, W. (2019), "Transport and retention of reduced graphene oxide materials in saturated porous media: Synergistic effects of enhanced attachment and particle aggregation", *Environ. Pollut.*, **247**, 383-391. <https://doi.org/10.1016/j.envpol.2019.01.052>.
- Xu, N., Cheng, X., Zhou, K., Xu, X., Li, Z., Chen, J., Wang, D. and Li, D. (2018), "Facilitated transport of titanium dioxide nanoparticles via hydrochars in the presence of ammonium in saturated sands: Effects of pH, ionic strength, and ionic

- composition”, *Sci. Total Environ.*, **612**, 1348-1357. <https://doi.org/10.1007/s11051-015-2972-y>.
- Zhang, M., Bradford, S.A., Simunek, J., Vereecken, H. and Klumpp, E. (2018), “Roles of cation valance and exchange on the retention and colloid-facilitated transport of functionalized multi-walled carbon nanotubes in a natural soil”, *Water Res.*, **109**, 358-366. <https://doi.org/10.1016/j.watres.2016.11.062>.
- Zhang, T. (2012), “Modeling of nanoparticle transport in porous media”, Ph.D. Dissertation; The University of Texas at Austin, Austin, U.S.A.
- Zhe, Z. and Yuxiu, A. (2018), “Nanotechnology for the oil and gas industry - an overview of recent progress”, *Nanotechnol. Rev.*, **7**(4), 341-353. <https://doi.org/10.1515/ntrev-2018-0061>.
- Zhu, W., Bartos, P.J.M. and Porro, A. (2004), “Application of nanotechnology in construction - Summary of a state-of-the-art report”, *Mater. Struct.*, **37**(273), 649-658. <https://doi.org/10.1007/BF02483294>.
- Zingg, R. and Fischer, M. (2019), “The rise of private-public collaboration in nanotechnology”, *Nano Today*, **25**, 7-9. <https://doi.org/10.1016/j.nantod.2019.01.002>.

CC

Symbols

A	Hamaker constant [J]
a_p	Particle radius [nm]
D	Particle diffusion coefficient [$\text{cm}^2 \cdot \text{s}^{-1}$]
k_{att}	Attachment coefficient [s^{-1}]
k_{det}	Detachment coefficient [s^{-1}]
N	Fluid-phase particle number concentration [$\# \cdot \text{L}^{-1}$]
s	Surface to surface separation distance [nm]
S	Solid-phase particle concentration [$\mu\text{g} \cdot \text{g}^{-1}$]
V_A	van der Waals attractive energy [J]
V_B	Born repulsive energy [J]
V_R	Electrostatic repulsive energy [J]
v_0	Fluid velocity [$\text{m} \cdot \text{hr}^{-1}$]
ε	Porosity [-]
$\varepsilon_0 \varepsilon_r$	Permittivity in water [$\text{C}^2 \cdot \text{J}^{-1} \cdot \text{m}^{-1}$]
κ	Inverse characteristic length of diffuse layer [nm^{-1}]
λ	Characteristic wavelength [nm]
ρ_b	Bulk density [$\text{g} \cdot \text{cm}^{-3}$]
ρ_p	Particle density [$\text{g} \cdot \text{cm}^{-3}$]
Ψ_{df}	Surface potential of a media [mV]
Ψ_{dp}	Surface potential of a particle [mV]